IEEE Access
Multidisciplinary | Rapid Review | Open Access Journal

Received 24 September 2022, accepted 10 October 2022, date of publication 19 October 2022, date of current version 26 October 2022.

Digital Object Identifier 10.1109/ACCESS.2022.3215639

RESEARCH ARTICLE

A Novel Enhanced VGG16 Model to Tackle Grapevine Leaves Diseases With Automatic Method

SEYEDAMIRHOSSEIN MOUSAVI[1] AND GHOLAMREZA FARAHANI[2]

[1]Department of Mechatronics, Karaj Branch, Islamic Azad University, Karaj 3149968111, Iran

[2]Department of Electrical Engineering and Information Technology, Iranian Research Organization for Science and Technology (IROST), Tehran 3313193685, Iran

Corresponding author: Gholamreza Farahani (farahani.gh@irost.org)

ABSTRACT Diseases of grape leaves are destructive because they spread very quickly. Therefore, they should be detected and tackled fast. This study proposes a novel Enhanced VGG16 model for detecting, identifying, and classifying three widespread diseases in grape leaves. These diseases include Downey Mildew, Anthracnose, and Powdery Mildew. The data are automatically gathered with the assistance of photos taken with a quadcopter from the grapevine garden. The main central system analyzes the images received from the quadcopter to identify diseases. If it finds any of the three diseases, it sends the command to the hexacopter to spray pesticide into the grapevine garden location where the disease is found. The proposed method using the Enhanced VGG16 model with Faster Region-based Convolutional Neural Networks (R-CNN) is compared with different networks, including VGG16, GoogLeNet, ResNet50, and AlexNet. The experimental results on the grape leaf diseases demonstrated that the proposed method achieves the mean Average Precision) mAP (criterion improvements of 0.53%, 0.912%, 2.759%, and 7.268% compared with the ResNet50, VGG16, GoogLeNet, and AlexNet networks, respectively. Also, the average accuracy of the proposed Enhanced VGG16 model is 99.6%, which is 0.437–1.91% higher than other models. The Enhanced VGG16 has the best precision, and the number of layers is acceptable, although it is not less.

INDEX TERMS Grapevine leaves diseases, faster R-CNN, quadcopter, hexacopter, VGG16.

I. INTRODUCTION

Diseases of garden trees can be a major problem for farmers. It can reduce the quality and quantity of the product, shorten the life of trees, and cause heavy economic damage to farmers and even the country's economy. Farmers can identify these diseases and eliminate them using a particular pesticide in the first stage. However, many human resources are required in extensive gardens. Therefore, it is time-consuming and costly.

Moreover, constant exposure to these decongestants causes diseases in the person. Among other problems, rainfall after each spraying stage can create the need for repair, and because of the high cost of pesticides, the garden requires great care and sensitivity. Therefore, by performing accurate and regular tracking operations, these harmful factors should be identified and implemented with a practical and managed program with the minimum consumption of pesticides. There are diseases in all parts of agriculture of ornamental flowers [1], apple trees [2], walnut trees [3], and cherry trees [4], even in vineyards. These diseases appear on the leaves of tree trunks and even the fruit of these trees. But today, in the agricultural sector, grapes are an essential horticultural crop with a production of about 75 million tons per year [5]. It is one of the most common fruit crops globally, and Iran, with an annual harvest of 3 million and 167 thousand tons of grapes, has ninth place in producing this product globally. Therefore, this product is of great importance in Iran [6]. The grapes garden is prone to diseases, which are very destructive for grapes because they spread very quickly, and after the disease progresses, the treatments become ineffective [7]. It is

The associate editor coordinating the review of this manuscript and approving it for publication was Jiachen Yang.

necessary to monitor the grapevine continuously to prevent diseases.

The use of pesticides on agricultural land today is associated with environmental problems and the risk of contamination by workers. Also, pesticide prices are very high, and their use is associated with limitations. Therefore, UAVs for imaging and spraying pesticide treatment on the diseased part of the vineyard significantly reduce the risk of waste of pesticides and contamination of workers. Also, this strategy is cheaper and faster than agricultural machinery and easy to control UAVs with higher planning and accuracy than the workforce, and efficiency will increase [8], [9].

Controlling the diseased leaves during the growing stages of crops is a crucial step. The disease detection, classification, and analysis of diseased leaves at an early stage, as well as possible solutions, are always helpful in agricultural progress. Paymode and Malode proposed the Convolutional Neural Network (CNN) method to detect Multi-Crops Leaf Disease (MCLD). The feature extraction of images using a deep learning-based model classified the sick and healthy leaves. The CNN-based VGG model was used for improved performance measures [10].

Also, a system was proposed to present an online machine learning-based papaya disease [11]. In this system, a person captures an image via a mobile application, sends it for disease detection, and compares some algorithm's accuracy: random forest, k-means clustering, Support Vector Clustering (SVC), and CNN. The system processed the images and gave feedback. This intelligent system can easily detect diseases with high accuracy of about 98.4% to predict papaya diseases. Nesteruk et al. applied machine learning for the plant classification of decompressed images with 92.6% accuracy on an 18-classes dataset. Their approach was promising for several agriculture-related applications, including plant classification, disease identification, and phenology deviation [12].

In Section II, the diagnosis of the grapevine diseases will describe. Section III expresses the related work. Grape leaf disease classes are presented in Section IV. The proposed method is described in Section V. The experiment results and comparison with other methods are reported in section VI. Finally, section VII concludes the paper.

II. DIAGNOSIS OF GRAPEVINE DISEASE

There are two main categories for diagnosing vineyard disease:

A. HUMAN DIAGNOSING

This task should be performed by human resources professionals with sufficient expertise in the field [13], but this is very time-consuming and costly and limits ongoing monitoring. This method has motivated many researchers to address these problems.

B. MACHINE DIAGNOSING

Various devices are used for machine monitoring, which include the following:

1) MECHATRONIC MACHINE

A mechatronic machine can move in the vineyard and take the leave's images using the camera mounted on the robot arm. Then, with image processing, the disease will be recognized. Finally, the pesticide of that disease was sprayed into the area where the disease occurs [14]. Also, Hashemi-Beni and Gebrehiwot proposed an autonomous vehicle to collect images from an organic carrots field and used U-net and convolutional neural networks to classify crop and field weeds [15]. Herrera et al. [16] presented different models to define the best model structure for the vehicle to use in agricultural tasks. The proposed vehicle was a quadricycle that has been modified and adapted with the best model to work autonomously for agricultural tasks.

The Dino robot to use for vegetable fields was designed by Naïo Technologies. Dino robot was operated autonomously with the help of RTK GPS and a camera. The robot has performed weeding one bed after another without human intervention, and after finishing the work, it sends a text message on the smartphone [17]. Another autonomous robot called 'Vitirover' utilized solar power for the electrical motors, which could work for hours without any pause that the French Company developed. This was used for cutting grass and weeds in vines [18].

Ecorobotix robot was operated automatically to cover the ground by getting its bearings and positioning itself with the help of its camera and GPS. Its vision system helped follow crop rows and detect the presence of weeds in and between the rows. Finally, two robotic arms sprayed a micro-dose of herbicide, systematically targeting the weeds that had been detected [19].

2) UNMANNED AERIAL VEHICLE (UAV)

As shown in Fig. 1, UAVs are generally divided into fixed and rotary wing categories. Fixed wings are like airplanes [20], and rotating wings are divided into two categories, which include helicopters [21] and Multi-rotors, which are named based on the number of rotors they possess, such as a quadcopter, meaning four rotors [22]. The hexacopter has six rotors [23], and the octocopter has eight rotors [24].

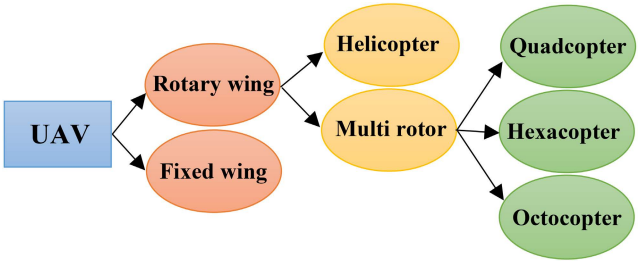

FIGURE 1. UAV platform types.

Today, with the advancement of quadcopter science, their unique design, compared to a helicopter, has a more stable flight and can be controlled by adjusting the speed of four

engines [25]. The quadcopter also has the characteristics of vertical takeoff and landing, liberty, etc. [26], [27].

Some quadcopters are about the size of a Compact Disc (CD). Some are wide as a meter, which is why quadcopters are widely used in many fields, such as safety control [28], military [29], rescue [30], agriculture [31], transportation [32], communications [33], meteorology [34], aerial photography [35] and other fields. With the modernization and development of technology, quadcopters will be developed immediately and have a wide range of applications in daily life [36]. However, quadcopters alone are not enough to solve disease problems in vineyards. Thus, with the advancement of science, it has become possible to image and measure different products [37].

Gennaro et al., with the use of UAVs, identified the infected areas of the vineyard using images taken by them from the top of the vineyard. Then, the disease was determined according to the color distinction created in that area [38].

Abdullahi and Sheriff [39] applied precision agricultural technology with a UAV embedded with optic and radiometric sensors to obtain high spectral resolution images of a plantation's status during a normal production/growth cycle. Then, farm image features were detected through the classification and optimization process to determine the plant's overall health status.

Today, image processing [40] is widely used in many fields, including the steel industry, metallurgy, exploration, fisheries, medicine, and transportation. Also, it is used in many industrial and mining companies in various agricultural sectors. In recent years, in the agricultural industry, drone has been used for several practical applications, such as calculating the number of organic fertilizers [41], monitoring biomass production [42], weeds [43], diagnosing diseases [44], spraying [45], etc.

Despite advances in such technologies, the automatic detection of symptoms using aerial imagery is challenging. Reference [46] was the first case that used aerial imaging drones. Still, much research has been carried out on diagnosing grapevine diseases in the vineyard.

Hexacopter [47] consists of six engines and six arms. The angle between each hexacopter engine is 60 degrees, and its shape is almost like a circle with six engines. Hexacopter is part of the family of multi-rotors that fly vertically. Also, six motors instead of four in quadcopters have given a much softer flight with more stability. They can be used to carry relatively heavier loads than quadcopters. Hexacopters were used in photography and mapping [48], spraying gardens [49], and carrying heavy loads and goods [50].

In this paper, due to three different types of pesticides to treat the three mentioned diseases, the payload weight is a little high, and the stability in spraying the pesticide at predetermined points is essential. Therefore, for pesticide spraying, a hexacopter is used.

This paper detects and tackles grapevine diseases by linking the quadcopter and hexacopter. First, the quadcopter takes grape leaf pictures and transfers them to the main data center. Then, grapevine diseases identify with image processing using a proposed method. Finally, if the disease is detected after image processing, the hexacopter depends on the type of disease, moves to the stored disease's labeled position according to the quadcopter, and starts spraying the detected disease region.

III. RELATED WORK

There are several methods for diagnosing grape diseases using image processing. Sannakki et al. [51] had an opinion on diagnosing grape diseases based on the Artificial Neural Network (ANN). Kaur and Kang [52] published that implementing a Support Vector Machine (SVM) is proper for detecting grape diseases. Firstly, the original image was captured, and then it was used for processing. Secondly, it gave the image's black and background pixels segmented image and separated the hue and saturation parts of the picture. Thirdly, the type of disease and the diseased portion of the image were detected, and the healthy part was segmented. Zhu et al. [53] have proposed an automatic detection method for grape leaf diseases based on image analysis and the Back Propagation Neural Network (BPNN) method. The Wiener filtering method based on wavelet transform was applied to eliminate the noise in the disease images. The grape leaf disease regions were segmented by the Otsu method, and morphological algorithms were used to improve the lesion shape. Finally, the Prewitt operator was utilized to extract the complete edge of the lesion region.

Other research identified and classified diseases in grape leaves using Artificial Bee Colony (ABC) based feature selection [54]. Initially, the input images were applied with pre-processing steps, which eliminated the noises and background of the photos.

Then, the features of color, texture, and shape were extracted. ABC-based attribute selection was used to find the optimal feature set. Finally, the selected features were given to the SVM classifier for foliar disease detection of grapes. The method was compared with the other feature selection algorithms.

Gao et al. [55] examined to check the potential use of hyperspectral imaging for non-destructive detection of Grapevine Leaf Roll-Associated Virus 3 (GLRaV-3) during the asymptomatic and symptomatic stages of Grapevine Leafroll Disease (GLD) in red-berried wine grape (Vitis vinifera) cultivar. Cabernet Sauvignon vines that tested positive and negative for GLRaV-3 were used in this study. Leaves from infected and non-infected vines were detached at five phenological stages. The hyperspectral imager acquired individual leaf images in the 2017, 2018, and 2019 seasons. The results indicated that the hyperspectral imaging technique could non-destructively detect virus-infected grapevines during asymptomatic stages.

In the system proposed by Adeel et al. [56], grapevine disease was identified with four steps. In the first step, a Local Contrast Haze Reduction (LCHR) enhancement technique was proposed to increase the symptom's local contrast. After

that, LAB color transformation was held in the second step, and the best channel was selected based on the pixel information later utilized in the thresholding function.

Then, the Canonical Correlation Analysis (CCA) approach extracted color, texture, and geometric features. At the time of feature fusion, the noise was added in the form of irrelevant and redundant features that were removed by Neighborhood Component Analysis (NCA). M-class SVM then performed the classification of final reduced features. The introduced system was assessed on the PlantVillage dataset of three types of grape leaf diseases: black measles, black rot, and leaf blight, including healthy.

Reference [57] presented an ML-powered mobile-based system to automate the process of plant leaf disease diagnosis. The developed system uses CNNs as an underlying deep-learning engine for classifying 38 disease categories. They collected an imagery dataset containing 96,206 images of plant leaves of healthy and infected plants for training, validating, and testing the CNN model.

Ahmed et al. [58] proposed a lightweight transfer learning-based approach to detect the diseases of tomato leaves. Their system has extracted features using a pre-trained MobileNetV2 architecture and a classifier network combination. Also, their system has replaced the traditional augmentation approaches with runtime augmentation to avoid data leakage and address the class imbalance issue. Evaluation of tomato leaf images from the PlantVillage dataset shows the effectiveness of their system.

Reference [59] used a fine-grained disease categorization method to solve the problem based on an attention network. In the classification model, the attention mechanism was used to increase identification ability. Also, an adversarial loss was applied to distinguish the generated image from the original image to suppress the noise introduced by the discrimination model. The compared results with the traditional classification network have shown the further enhancement of the identification accuracy of peach and tomato leaf diseases.

Also, an end-to-end deep learning model was developed to identify healthy and unhealthy corn plant leaves with better classification accuracy by Amin et al. [60]. The model utilized two pre-trained CNNs, EfficientNetB0, and DenseNet121, to extract deep features from the corn plant images. Then the deep features extracted from each CNN were fused using the concatenation technique to produce a more complex feature set from which the model to learn better about the dataset.

Elfatimi et al. [61] presented a method to classify beans leaf disease. The model was trained using MobileNetV2 architecture under some controlled conditions as MobileNet. The results showed that their MobileNet model achieves better classification performance for beans leaf disease than other methods.

In the other research, the proposed method efficiently identified grape leaf diseases using low-resolution images with an integrated LoRa and CNN-based computer vision system [62]. Finally, according to the visualization findings, the disease's spot region is highly activated. This is how the network distinguishes between different grape leaf diseases.

AlexNet [63] was the first CNN to win the ImageNet challenge in 2012. AlexNet's CNN consists of five convolution layers and three Fully Connected (FC) layers. There are 96 to 384 filters within each convolution layer, and the filter size is 3×3, 5×5, and 11×11, with 3 to 256 channels. A Rectified Linear Unit (ReLU) with non-linearity was used in each layer. Max-pooling of 3×3 was applied to the outputs of layers 1, 2, and 5. AlexNet used a stride of 4 at the first layer of the network. AlexNet's model requires 61M weights to process one 227×227 input image (top-5 error of 16.40%).

Google introduced the inception structure at the 2014 ImageNet Large-Scale Visual Recognition Challenge (ILSVRC14), called GoogLeNet [64].

GoogLeNet's model can achieve high accuracy by deepening the layers to increase the neural network's performance. At this model's core, the neural network's inner layer is extended to output various correlation distributions. It is based on the idea that the neural network output of each layer has optimal efficiency if various probability distributions with high correlations with the input data are obtained. In the basic inception v1 module, where input data are fed into four independent layers (1×1, 3×3, 5×5 convolution layers, and 3×3 max-pooling layer), the outputs are combined into a single data set.

Inside, the convolutional layers derive various spatial information from the input data. The maximum pooling layer extracts distinct features by reducing the channel and size of the input data. Therefore, the inception module is a method of extracting more information into a smaller layer by widening the layer of the neuron network, which is only composed of the existing depth. The VGG-Net [65] model reinforced that the CNNs must have a deep network of layers. ResNet [66], also known as Residual Net, used residual connections to go deeper. ResNet determined an object's exact location, a huge jump in CNNs. It is $8\times$deeper than VGG-Net with lower complexity and won the ImageNet challenge 2015 (top-5 error of 3.57%) with 152 layers.

IV. GRAPE LEAF DISEASE CLASS

There are various diseases in grape vineyards. Therefore, the diagnosis and treatment of these diseases are essential. The disease is very destructive for grapes because it spreads quickly, and treatments are generally ineffective after the disease progresses [7]. Usually, grape trees are studied for three Downey Mildew, Anthracnose, and Powdery Mildew diseases [35]. Therefore, this paper offers a solution to deal with them. In continuation, these three diseases are explained briefly.

A. DOWNEY MILDEW

Downy mildew usually appears as patches and spots on the leaf's upper and undersides. It is generally seen as a furry growth that forms under humid conditions. It is usually grey to light violet in color. The spores are spread by wind or rain

or by irrigation water. This disease relies on high relative humidity for growth, and the spores cannot germinate or grow under dry conditions [67]. Fig. 2 shows a leaf sample for this disease with a grey image and RGB channels.

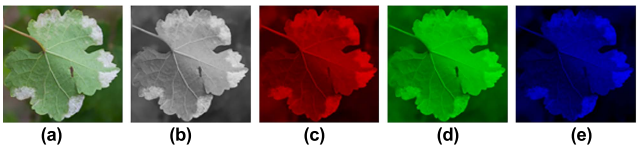

FIGURE 2. Downey mildew: (a) input image; (b) grey image; (c) red channel; (d) green channel; (e) blue channel.

B. ANTHRACNOSE

Anthracnose causes small brown spots on grape leaves that fall off when the tissue dies, creating a shot-hole effect. Young affected shoots become distorted and dieback. On stems, white-centered, bird's eye spots develop, which can grow and girdle the stem resulting in dieback. Young, rapidly growing leaves and stems are most affected. Diseased leaves, stems, and stem cankers are a source of disease later in the season and for disease the following year [68]. Fig. 3 shows a leaf sample for this disease with a grey image and RGB channels.

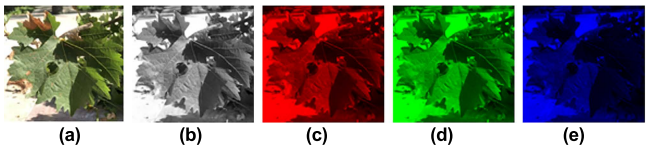

FIGURE 3. Anthracnose: (a) input image; (b) grey image; (c) red channel; (d) green channel; (e) blue Channel.

C. POWDERY MILDEW

Powdery mildew is a fungus that spreads a white or ash-grey film over the upper and lower surfaces of the leaves of plants. This disease usually occurs in the older leaves. Powdery mildew fungus favors humid and dry conditions. Often the appearance of a whitish film on leaves and buds will be evident. New growth is distorted, and older leaves become blackened. Flower buds may fail to open [69]. Lime Sulphur, Rose spray ready-to-use, and Rose spray concentrate could be used to cope with this disease. Fig. 4 shows the leaf sample for this disease with a grey image and RGB channels.

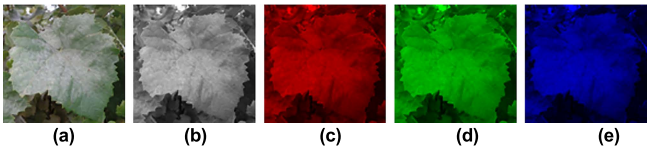

FIGURE 4. Powdery mildew: (a) input image; (b) grey image; (c) red channel; (d) green channel; (e) blue channel.

V. PROPOSED STRATEGY FOR DATA GATHERING TO TACKLE GRAPEVINE LEAVES DISEASES

Today, robots play an important role in people's lives [70]. This research aims to design a coordinated and mechatronic system. It includes the quadcopter, hexacopter, and main central system that communicate to identify and eliminate the three main diseases in the vineyard. As shown in Fig. 5, the quadcopter used in this paper had a 2Megapixel camera, wide-angle live video, gravity sensor, 3Wh Li-ion 3.7V 860mAh battery, and VK16E GMOUSE GPS module to save the latitude, longitude, and elevation of the taken picture.

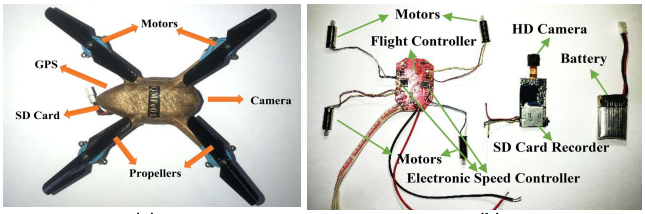

FIGURE 5. Quadcopter: (a) outside part; (b) inside parts.

One of the features of this quadcopter was its flexibility and stability in flight. Because of these features make it easy to fly down, back, and forth, sideways, and horizontally. This quadcopter was equipped with an MPL3115A2 sensor for measuring flight altitude. It had an HD camera in front that saved captured images with a resolution of 1920×1080 pixels in JPEG format and its position in the RAM.

The body of the quadcopter and the propellers of the four engines changed to reduce the weight of the quadcopter and increase the flight time. Therefore, the quadcopter's weight reached almost half a kilogram, and its flight time increased from 10 minutes to 15 minutes. 2 LEDs on the front of the quadcopter were used for more brightness during photography, enabling the quadcopter to take photos well even in semi-dark environments.

As shown in Fig. 6, the hexacopter was an AGRAS T20 model with three types of pesticide in the tank for the diseases mentioned above. These pesticides were separated into a tank with a divider. It had about 20 kg weight and eight pesticide spray nozzles with a spray surface of 3 meters.

The other specifications of the hexacopter were 15 minutes flight time, IP 67, omnidirectional digital radar, real-time visual monitoring system, scheduling, flight route drawing, obstacle collision sensor, RTK module, and navigation from the map.

A. STAGES OF THE PROPOSED STRATEGY

In the first stage, the quadcopter began to fly according to a specific predetermined search pattern in the rows of vines. Then, it started photographing the leaves of the vines using a camera mounted on the quadcopter and automatically took these photos at a precise location.

In the quadcopter, two LEDs were used in front of it for more brightness when taking a photo in low light and not

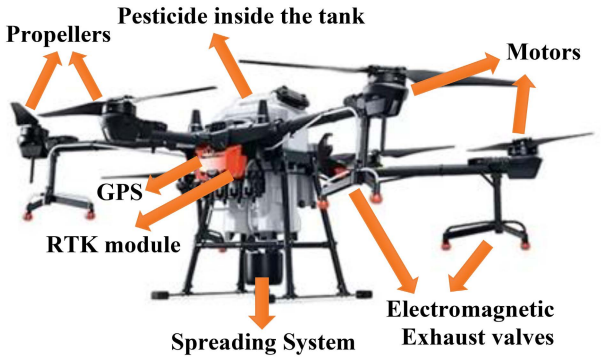

FIGURE 6. AGRAS T20 hexacopter.

at night. Generally, the photography of the quadcopter was different according to each season (due to the short day and night). The quadcopter was active from 10 am to 4 pm in this paper.

DGPS [71] has been used to increase the accuracy and reduce the error location of the quadcopter. With DGPS, the averaged position error was less than 10cm, so the leaf disease easily sprayed when the disease was detected in grape leaves.

Then the photos were loaded into a main central processing system containing reference images. These reference images were 10,000 RGB photos taken manually from a vineyard near Shahriar city in two years (2018-2019) by a Kinect V2 sensor located 0.5 meters from the vine trees at 30cm and 45cm heights. They were taken at different times of the day when the sunlight was changed. Their dimensions were 1920×1080 pixels.

All images were entirely taken manually, labeled, and stored in a separate file to improve the robustness of the proposed method. From these 10,000 images, 8000 images were used for training and 2000 for testing. The annotated images were augmented using geometric transformation and image enhancement. All images were used as the inputs to Faster R-CNN-based Enhanced VGG16 (proposed method), AlexNet [63], GoogLeNet [64], VGG16 [65], and ResNet [66] model for training and testing.

The test dataset included an equal number of images (500 images) for every three diseases and 500 images for healthy leaves. To diagnose the grapevine disease accurately, if the symptoms of a particular disease were detected, the proposed method identified the exact type of disease.

Then the main central system, after identifying the type of disease, sends a command to the hexacopter. The command contains information about the location and type of disease, height above ground level, and leaf direction to the north or south. The hexacopter starts flying from the parking lot and flies to the location sent from the central system. It sprays the target area for 20 seconds with proper pesticide according to the command from the central system that the pesticides are in the tank on the hexacopter.

After spraying, a message containing the completion of the work is sent to the main central system, and the hexacopter returns to its original parking lot. Then after the duration, depending on the type of disease, the operator commands the quadcopter to recheck the vineyard. The connection between the quadcopter, hexacopter, main central system, and the operator is shown in Fig. 7.

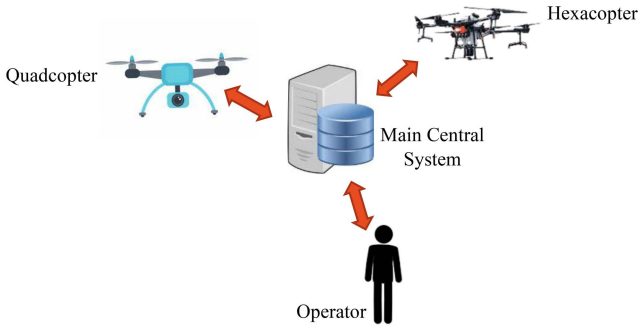

FIGURE 7. The main central system establishes the connection between the quadcopter, hexacopter, and operator.

B. QUADCOPTER MOVEMENT PATTERN IN THE VINEYARD

As shown in Fig. 8, grape trees were planted in columns 100 meters long and 1 meter wide for easier access and irrigation in the field where this system was tested. Similarly, the movement pattern of the quadcopter was programmed to fly and take pictures along these columns of vines, which can be changed according to the planting of different types of plants. According to Fig. 8, the quadcopter started flying from one side, took photos, and passed through the columns to reach the end of the vineyard. The height of the quadcopter from the ground was programmable (generally between 0.5 meters to 2 meters). Also, the distance of the quadcopter from the grape leaves was between 1 and 2 meters. This distance is suitable for taking a photo and preventing the quadcopter from colliding with the leaves to damage them.

The maximum speed of the quadcopter was 60 km/h. After reaching the quadcopter at the vineyard, it took a photo at a speed of 2 m/s. The photos were taken at a distance of about 1.5 meters from the grape trees with a height of about 1 meter. Therefore, according to the quadcopter's speed, in a 15-minute flight, assuming a 1-minute round-trip flight from the parking lot, it can take a photo in about 14-minutes per flight, which covers an area of about 0.4 hectares.

The number of photos is limited to the capacity of RAM usage in the quadcopter. The time interval between taking photos was adjustable. In a 15 minutes flight (1-minute round trip flight from the parking lot to the vineyard plus a 14-minute flight on the vineyard), with four photos per second, the required RAM was equal to 6,967,296,000, which was supported with an 8 GB RAM. If a shorter time interval for taking photos is considered, this goal can be achieved by increasing the RAM. Fig. 9(a) shows an operation of the quadcopter during its mission to take photos of leaves in a vineyard.

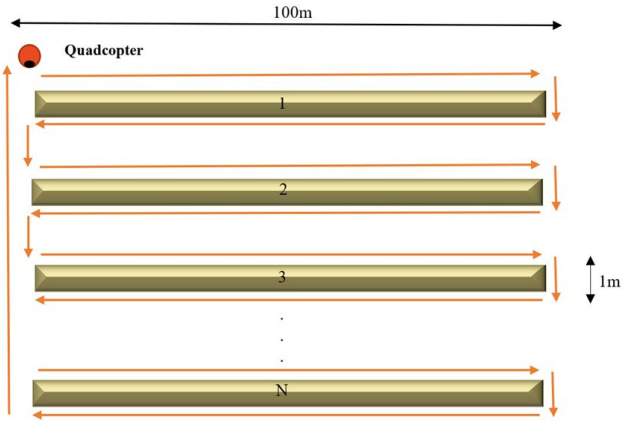

FIGURE 8. Quadcopter movement pattern in the vineyard shown with arrows.

Hexacopter was used to spray areas whose images had been provided to the main central system by a quadcopter, and this system diagnosed grapevines in those areas as diseased. Therefore, the time of the hexacopter for spraying was not too long because it would fly on a case-by-case basis if the disease was diagnosed. Concerning the hexacopter speed, the round-trip flight from the parking lot to the vineyard was about 1.5 minutes. Fig. 9(b) shows the hexacopter spraying the pesticide on the vineyard.

FIGURE 9. Operation of (a) quadcopter, (b) hexacopter.

C. FLOWCHARTS OF THE OPERATIONS

A flowchart of the quadcopter operation is shown in Fig. 10. Also, the main central system and hexacopter operations are shown in Fig. 11 and Fig. 12, respectively. According to Fig. 10, first, the quadcopter flies from the parking lot. Then it starts to take a photo and save it with its location in the RAM. The quadcopter continues its flight and takes other pictures to reach the end of the vine's rows. Based on Fig. 11, the image is analyzed with the proposed method to find the disease after uploading the taken image by a quadcopter into the main central system. If the analysis results conclude the disease, the command will send to the hexacopter to start the movement for pesticide spraying. Finally, as shown in Fig. 12, the operation of the hexacopter starts. Based on the sent command from the main central system resulting from the proposed method analysis, the hexacopter gets the pesticide spraying mission with the type of disease and location. After pesticide spraying, if the main central system sends another

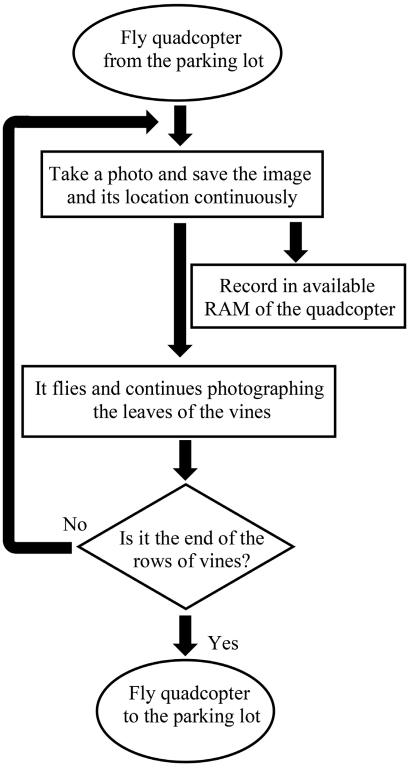

FIGURE 10. Quadcopter operation flowchart.

location, the hexacopter continues its mission; otherwise, it flies back to the parking lot.

D. DATA AUGMENTATION

Whereas increasing the number of training images using data augmentation, one could prevent overfitting or non-convergence of the deep learning algorithm [72]. Data augmentation, including geometric transformation and data enhancement, was implemented using the software Matlab 2020a with the Image Processing Toolbox in the proposed method. The Matlab function "imrotate" was used to rotate the raw image, and 90°, 180°, and 270° of rotation were achieved by changing the function parameter "angle".

If the object's color has low contrast and brightness with the background of the image, then the color information is not enough to find the object in the image [73]. The enhanced images can improve the detection performance of the neural network by correctly identifying the diseased leaves of different orientations. Multiplying a proportional coefficient near 1.0 by the original image, RGB can adjust the value of each component to make the image brightness higher or lower [74]. When taking the photo at night (low light) or during the day (high light), bounding boxes will be difficult to draw during manual annotation because the edge of the target is unclear. Four proportional coefficients of 0.7, 0.8, 1.1, and 1.2 were selected based on the target edge, as shown in Fig. 13, which can be accurately identified during manual annotation. If, after multiplying these coefficients, the resulting number

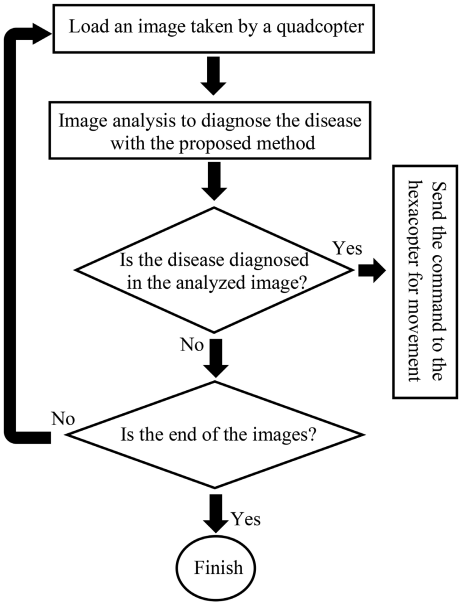

FIGURE 11. Main central system operation flowchart.

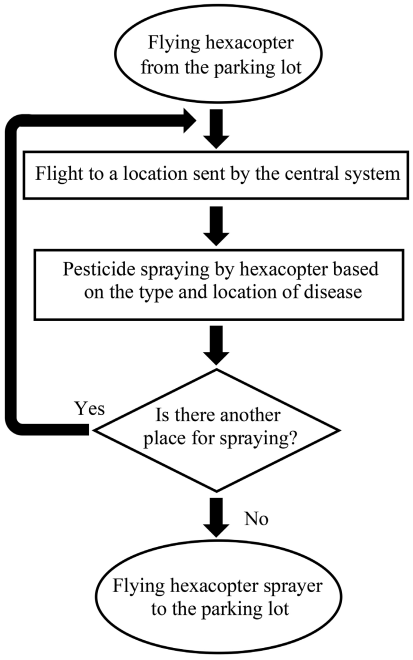

FIGURE 12. Hexacopter operation flowchart.

increased by 255, then the same number, 255, applies. The histogram matching method has also been used to improve the quality of training sample images [75].

The camera may shake and have incorrect focus, which causes the image to be blurred, and thus difficult to detect. Therefore, the Matlab function 'imfilter' is used to blur the images with the generated filter in the training stage. The blurry image was used four times to make the convolutional network model adaptable completely to the blurred images.

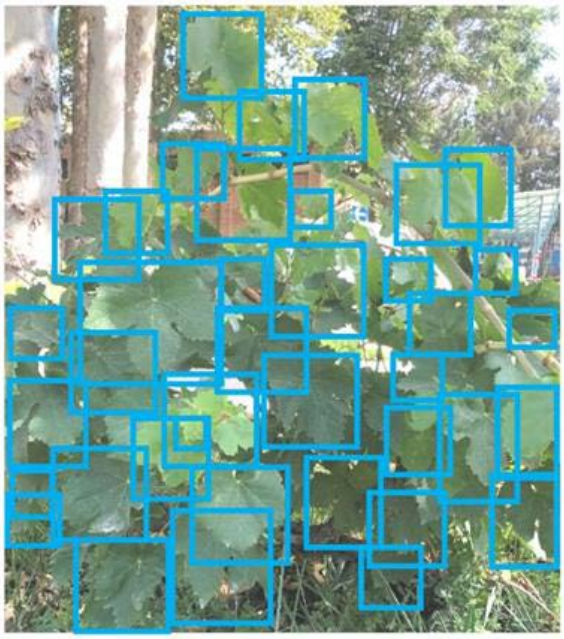

FIGURE 13. Sample of bounding boxes drawn accurately with the proposed method (The photo is taken automatically with a quadcopter).

E. DEEP LEARNING MODEL

The Faster R-CNN deep learning model [76] has widely been used in agriculture, especially in identifying fruits, and it had good results. The Faster R-CNN model merges Region Proposal Network (RPN) object classification and localization into one unified deep object detection network. The RPN generates the proposals, and the Faster R-CNN was used to accurately locate the object [77].

The RPN, a fully convolutional neural network, uses a partial convolutional layer of the VGG16 network to generate a feature map of a leaf's image. It outputs a series of leaves target candidate regions [78].

An $n \times n$ sliding window is used to scan the feature map of the leaves image, and m target candidate regions are predicted for the position of each sliding window. The m proposals for the same localization are called anchors. An anchor point is in the center of the sliding window and is related to scale and aspect ratio [79]. In the proposed method, $n = 3$, therefore $m = 9$ anchors. Two fully connected layers of the same level regression and classification layers follow 512-dimensional features.

The RGB image was used as the input of VGG16 [65] and then processed by the network. The network performed a random gradient descent method on the image blocks to update the parameters. A filter of size 3×3 with stride one was used to construct a convolutional layer by VGG16, where the padding parameter in the same convolution was used as its parameter.

Then a 2×2 filter with stride two was used to build the max-pooling layer. The feature map of the image was extracted through convolution, ReLU, and pooling

operations, which were shared in the subsequent RPN layers and fully connected layers.

1) PROPOSED METHOD

As shown in Fig. 14, the proposed grape leaf disease detection method is based on Faster R-CNN with an Enhanced VGG16 model. The dark blue, red, blue, green, and grey layers correspondingly represent the full connection, convolutional, pooling, ReLU, and binary layers.

The proposed Enhanced VGG16 model consists of 14 convolutional layers, five pooling layers, six Batch Normalization (BN) layers, and one fully connected layer. The following changes have been made to reach the Enhanced VGG from the VGG model. The Fc6 and Fc7 fully connected layers were removed from the VGG16 model. Conv6 and Global Average Pooling (GAP) layers were added to the VGG16 model. The two fully connected layers, Fc6 and Fc7, in the VGG16 fully connected each neuron with all the neurons in the previous layer.

Therefore, they generate many parameters and occupy many computing resources. Reference [80] proposed a GAP for discarding these two fully connected layers. The GAP can be replaced with a fully connected layer. Experiments demonstrated that GAP could reduce the number of parameters, the volume of calculation, and the overfitting in the model [80].

GAP calculates the mean value of the pixel points in each feature map, outputs a feature point, fuses these feature points into feature vectors, and then enters them into the Softmax layer. Therefore, it reduces the number of parameters, the volume of calculation, and the overfitting.

Also, GAP can output a feature graph for each category, which directly endows features with real meaning and more intuitively connects each category and feature graph. For confirmation of GAP's function, many advanced network models, such as GoogLeNet, and ResNet, have introduced a GAP.

In this paper, a convolutional layer Conv6 with a convolution kernel size of 1×1 has been placed in front of the added GAP to optimize the VGG16 model further. The effect of the number of filters on the model performance has been analyzed by setting various 128, 256, and 512 filters during model construction. Conv5 of the VGG16 network model has been changed to a deeply tandem group. VGG16 model continues the simple network structure of classical models such as AlexNet.

The deeply tandem group has expanded the deep network to improve its performance. But compared with some sophisticated advanced networks, the network model structure is single, and the model complexity is too low, making it challenging to deal with complex tasks. In this paper, using the inception structure of GoogLeNet [64], the three convolutional layers of the VGG16 network model Conv5 were transformed into a deeply tandem group.

As shown in Fig. 15, the input characteristics all passed to each convolutional layer in the improved Conv5 structure. This structure did not produce the wastage of the decreasing step-by-step, which could increase the complexity of the model to a certain extent and improve the width of the network. Therefore, it made conv5 learn more characteristics, enhanced the identification accuracy of the network, and affected model optimization.

The BN layers were added in the proposed Enhanced VGG16 [81]. The BN process pulls the input values in neural network neurons back to the standard normal distribution, where the mean value is 0, and the variance value is 1. With this operation, input values place in the input-sensitive areas of non-linear function pairs. Therefore, small changes in the input value can significantly impact the loss function, and the gradient can be increased to prevent the problem of gradient disappearance. Also, the training and convergence speed of the model can be significantly accelerated. It has been proven that adding the BN layers to network models has a significant benefit, but it is unclear where BN should be placed on the network.

First, in 2015, BN was added to the front of the ReLU layer. Nevertheless, some researchers have suggested that putting the BN layer after the ReLU layer is better.

Reference [82] stated that putting the BN layer in front of the ReLU layer sometimes hurts the model, whereas increasing the number of training images using data augmentation could prevent overfitting or non-convergence of the deep learning algorithm. Placing the BN layer after the ReLU layer improves accuracy and reduces loss. Therefore, in the proposed method in this paper, the BN layer was placed between the ReLU layer and the model's pooling layer to obtain the best results.

2) NETWORK TRAINING

The training platform included a computer with an Intel Xeon E7-8891 (3.50 GHz) ten-core CPU and a GPU of NVIDIA TITAN Xp Graphics Card 12GB (3584 CUDA cores) and 32GB of memory running on a Windows 10 64-bit system. The software tools included CUDA 11.4, cuDNN 8.0, Python 3.9, and Microsoft Visual Studio 16.0. The experiments were implemented in the TensorFlow framework. The RPN was implemented as a fully convolutional network. It was optimized through an end-to-end using backpropagation and mini-batch gradient descent. The specific steps of training were as the following. A fixed value of 0.9 was set as the network's momentum, and 0.0005 was used as weight decay. Mini batches of 8000 images were used to train the model. The constant learning rate of 0.001 was chosen for all layers in the network, and 100,000 iterations were selected to analyze the training process.

VI. EXPERIMENTAL RESULTS

In this section, the experimental results are described. First, the criteria for the evaluation of the proposed method are expressed. Then the results of the proposed method with different recent methods are compared.

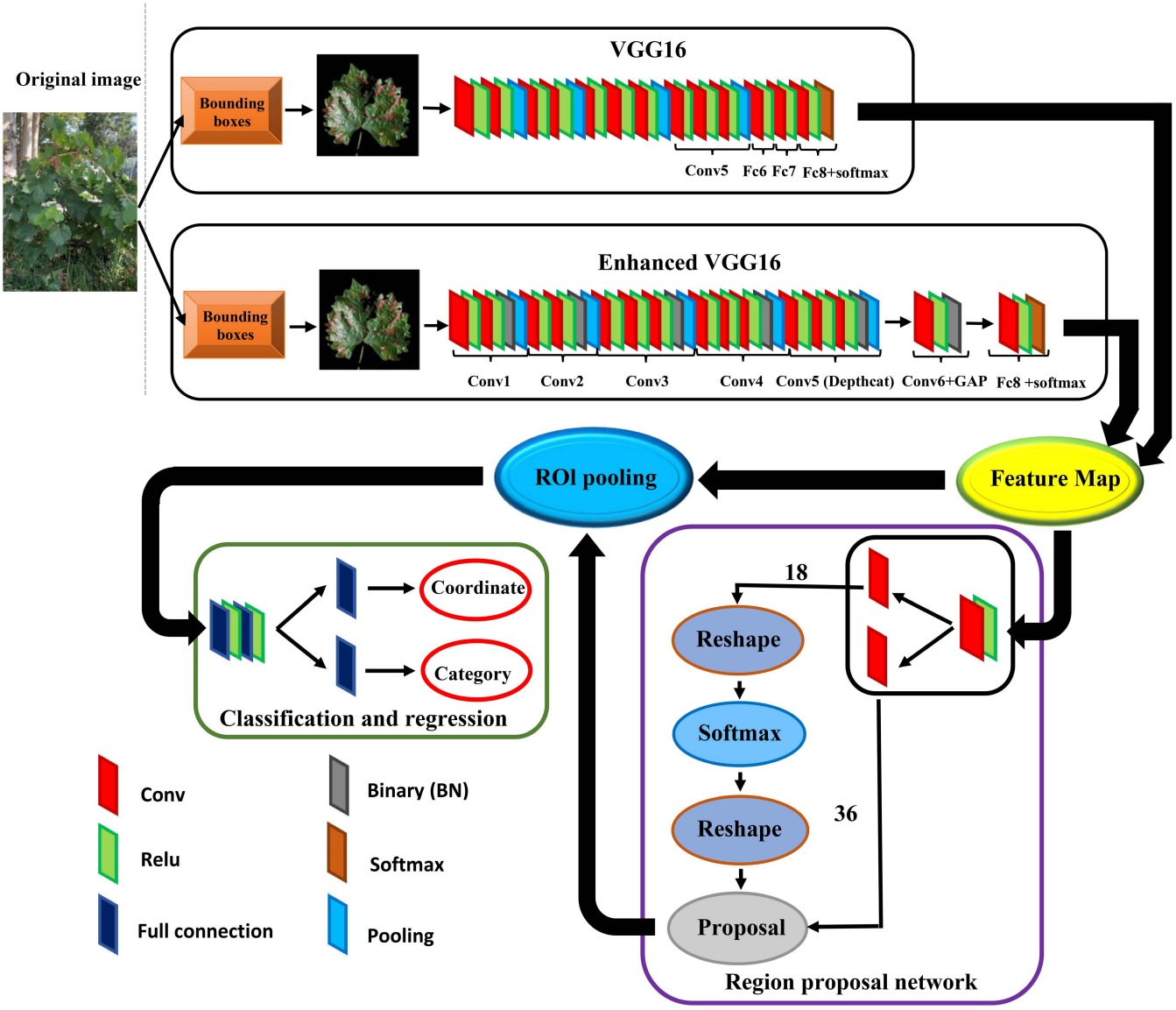

FIGURE 14. The proposed disease grape leaf detection method is based on Faster R-CNN with an Enhanced VGG16 model.

A. CRITERIA

Accuracy, Precision, and Recall are essential values for image processing and object detection. Accuracy represents the proportion of all correctly identified samples to the total. It is a very intuitive evaluation index, but sometimes it can be deceptive. When the number of samples is unbalanced, the accuracy value favors more samples.

Precision refers to the proportion of correctly classified and located categories to the total returned results in the turned results. The recall rate refers to the proportion of correctly classified and located categories in the returned results to the total related categories.

The evaluation criteria in this paper are mAP [83], Precision, Accuracy, Precision, and Recall.

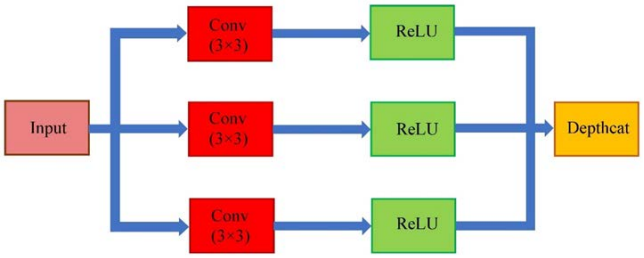

FIGURE 15. Improved Conv5 structure diagram.

The Accuracy, Precision, and Recall are defined in (1), (2), and (3), respectively.

$$\text{Accuracy} = \frac{\text{TP} + \text{TN}}{\text{TP} + \text{TN} + \text{FP} + \text{FN}} \tag{1}$$

TABLE 1. Multi-class grape leaf disease detection.

Network type	AP				mAP	Model Size (MB)	Layer	Parameters (Million)	Training Time (Hours)
	Disease			Healthy leaves					
	Downey Mildew	Anthracnose	Powdery Mildew						
VGG16 [65]	0.982	0.992	0.991	0.984	0.98725	516	41	138	6.35
GoogLeNet [64]	0.971	0.983	0.971	0.953	0.96950	28	144	7	2.24
ResNet50 [66]	0.991	0.993	0.992	0.988	0.99100	97	177	23.6	4.38
AlexNet [63]	0.962	0.919	0.887	0.947	0.92875	225	25	60	5.34
Enhanced VGG16 (Proposed method)	0.994	0.998	0.996	0.997	0.99625	53.2	45	14.2	3.53

TABLE 2. Improvement percentage of mAp for Enhanced VGG16 compared to other networks.

Network	AP improvement(%)				mAP *(%)*
	Disease			Healthy leaves	
	Downey Mildew	Anthracnose	Powdery Mildew		
VGG16	1.222	0.605	0.505	1.321	0.912
GoogLeNet	2.369	1.526	2.575	4.617	2.759
ResNet50	0.303	0.504	0.403	0.911	0.530
AlexNet	3.326	8.596	12.290	5.280	7.268

TABLE 3. Multi-class grape leaf disease detection.

Network type	Accuracy (%)			
	Disease			Average
	Downey Mildew	Anthracnose	Powdery Mildew	
VGG16	98.35	97.95	98.15	98.1500
GoogLeNet	97.00	98.15	98.05	97.7333
ResNet50	98.90	99.10	99.50	99.1667
AlexNet	97.50	98.05	97.75	97.7667
Enhanced VGG16 (Proposed method)	99.50	99.75	99.55	99.6000

TABLE 4. Improvement percentage of *Accuracy* for enhanced VGG16 compared to other networks.

Network	Accuracy improvement (%)			
	Disease			Average
	Downey Mildew	Anthracnose	Powdery Mildew	
VGG16	1.169	1.838	1.426	1.477
GoogLeNet	2.577	1.630	1.530	1.910
ResNet50	0.607	0.656	0.050	0.437
AlexNet	2.051	1.734	1.841	1.875

$$\text{Precision} = \frac{\text{TP}}{\text{TP} + \text{FP}} \tag{2}$$

$$\text{Recall} = \frac{\text{TP}}{\text{TP} + \text{FN}} \tag{3}$$

where True Positive (TP) represents the number of positive samples classified correctly in the prediction result, False Positive (FP) represents the number of negative samples for which the prediction result is incorrectly detected, True Negative (TN) expresses the number of positive samples classified incorrectly in the prediction result, and False Negative (FN) represents the number of undetected positive samples in the prediction result.

The Precision-Recall curve can be drawn with the Precision as the ordinate and the Recall as the abscissa. The Average Precision (AP) is the area under the Precision-Recall curve; therefore, the integral of the Precision-Recall curve is the AP as (4).

$$\text{AP} = \int_0^1 p(r)d \tag{4}$$

The Recall is divided into n blocks $\left[0, \frac{1}{n}, \ldots, \frac{n-1}{n}, 1\right]$, and the mAP is determined by the average value. If there are N categories in total, the mAP is calculated using (5).

$$\text{mAP} = \frac{\sum_{n=1}^{N} \text{AP}(n)}{N} \tag{5}$$

B. COMPARED METHODS

In this section, the proposed method is compared with other related methods.

1) MAP CRITERION

The mAP value of Multi-class grape leaf disease detection results for Enhanced VGG16 (proposed method), VGG16, GoogLeNet, ResNet50, and AlexNet methods are expressed.

The proposed method has achieved the mAP of 0.99625 for the three disease classes, the best value among other networks.

The mAP of the ResNet50, VGG16, GoogLeNet, and AlexNet are 0.99100, 0.98725, 0.96950, and 0.92875 respectively. The layers of the different networks are expressed in the last column of Table 1.

Table 2 shows the percentage improvement of the mAP for VGG16, GoogLeNet, ResNet50, and AlexNet networks compared to the Enhanced VGG16 (proposed method), which has the best mAP.

Based on Table 2, the proposed method has the mAP improvement of 0.53%, 0.912%, 2.759%, and 7.268% than ResNet50, VGG16, GoogLeNet, and AlexNet networks, respectively. Therefore, ResNet50, VGG16, and GoogLeNet are in the second, third, and fourth ranks. The worst result is for AlexNet. From another point of view, the proposed Enhanced VGG16 model has improved the mAP of the VGG16 model by 0.912%, which is an acceptable improvement.

2) ACCURACY CRITERION

Table 3 shows that the average accuracy of Enhanced VGG is 99.6%, which is 0.437–1.91% higher than other models (Table 4). The results showed that the Enhanced VGG method in each disease has better accuracy and the best average accuracy among other methods. The main reason for the better results is changing the VGG model (omitting some layers and adding new layers).

3) PRECISION CRITERION

The Precision-Recall curves achieved by Enhanced VGG16 (proposed method), VGG16, ResNet50, AlexNet, and GoogLeNet on the testing dataset are shown in Fig. 16. The Precision values of the proposed method are the highest, with the same Recall values for all diseases and healthy leaves.

The ResNet50 achieved the second-highest precision. VGG obtained a higher Precision for the three remaining networks than GoogLeNet and AlexNet on all three diseases

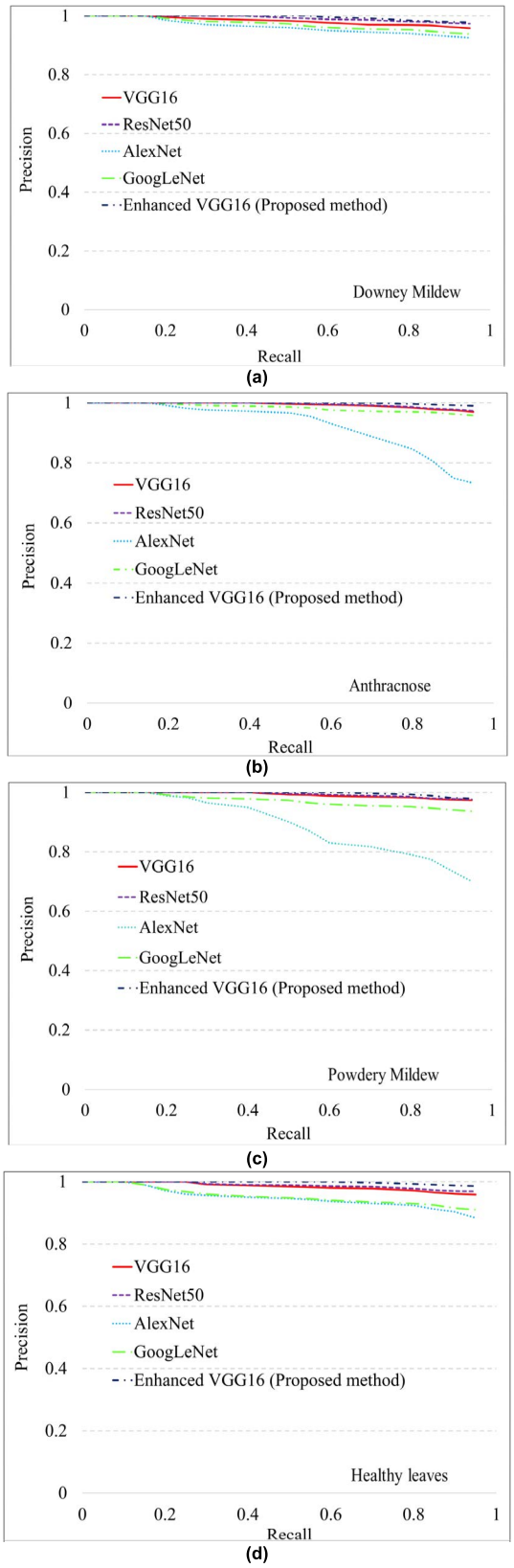

FIGURE 16. Precision-Recall curves of the models on the testing dataset with Enhanced VGG16 (proposed method), VGG16, GoogLeNet, AlexNet, and ResNet50: (a) Downey Mildew; (b) Anthracnose; (c) Powdery Mildew; (d) Healthy leaves.

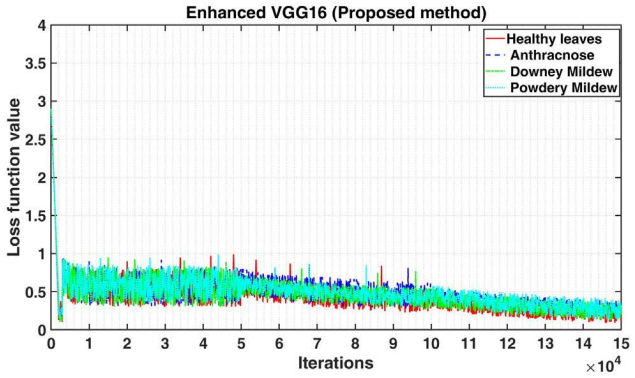

FIGURE 17. Test loss curve of enhanced VGG16 network (proposed method) for downey mildew, anthracnose, powdery mildew diseases, and healthy leaves.

and healthy leaves with the same Recall value. The lowest precision is for AlexNet.

4) MODEL SIZE, NUMBER OF PARAMETERS, AND TRAINING TIME CRITERIA

Table 1 expresses the model size and the number of parameters for Enhanced VGG16 (proposed method), VGG16, GoogLeNet, ResNet50, and AlexNet methods.

GoogLeNet has the smallest model size and parameters. Because the Enhanced method uses GAP; therefore the number of VGG16 parameters has reduced to 14.2 million for Enhanced VGG16.

As a result, the Enhanced VGG16 (Proposed method) ranks second in the lowest number of parameters. A deeper classifier may has a smaller model size and number of parameters depending on the classifier configuration.

The training time for different networks is shown in Table 1. Due to a higher number of parameters, the VGG16 model considerably requires the highest training time.

Enhanced VGG16 has the second rank in the lowest training time after GoogLeNet.

Fig. 17 Shows the results of the loss curve of the test set for 150,000 iterations of the Enhanced VGG16 network (proposed method), which has the best results among other networks. The variation trend for Downey Mildew, Anthracnose, Powdery Mildew diseases, and healthy leaves was almost overlapping.

The loss value decreases as the number of iterations increases but is generally stable when the number of iterations reaches 140,000 iterations, and the average loss value is 0.286. The results verify that the Enhanced VGG16 network learns the features appropriately with good convergence ability, achieving the desired results.

VII. CONCLUSION

Disease in the vineyard can be spread quickly and make a high loss. This paper considers three general diseases: Downey Mildew, Anthracnose, and Powdery Mildew. These diseases damage the leaves of grape trees.

The proposed method that is Enhanced VGG16 has been implemented for automatic diagnostics. It consists of the quadcopter to take a photo, the main central system to process the images, and the hexacopter to spray the pesticide based on the type of disease recognized by image processing and the saved location of the disease with the quadcopter.

The proposed method is based on Enhanced VGG16 with Faster R-CNN deep learning method. Also, different networks, including VGG16, GoogLeNet, AlexNet, and ResNet50, are compared with the proposed method to find the best network for disease detection in grapevine gardens.

Finally, this paper demonstrates that the proposed Enhanced VGG16 network with Faster R-CNN has the best mAP, accuracy, and precision among other networks. The number of layers for image processing in the proposed network is acceptable, although not less.

REFERENCES

[1] R. C. Lambe, "Ornamental and flower diseases: Camellia flower blight," Plant Dis. Control Notes, Extension Division, Virginia Polytech. Inst. State Univ., Tech. Rep., 1979, vol. 99.
[2] M. Mehrabi, E. M. Goltapeh, and K. B. Fotouhifar, "Studies on cytospora canker disease of apple trees in semirom region of Iran," *J. Agricult. Technol.*, vol. 7, no. 4, pp. 967–982, 2011.
[3] E. E. Wilson, F. M. Zeitoun, and D. L. Fredrickson, "Bacterial phloem canker, a new disease of Persian walnut trees," *Phytopathology*, vol. 57, no. 9, pp. 618–621, 1967.
[4] K. C. Eastwell and M. G. Bernardy, "Relationship of cherry virus a to little cherry disease in British Columbia," in *Proc. 17th Int. Symp. Virus Virus-Like Diseases Temperate Fruit Crops*, 1997, pp. 305–314, doi: 10.17660/ActaHortic.1998.472.36.
[5] F. Oiv, "Table and dried grapes: World data available," in *Proc. Int. Organisation Vine Wine*, Paris, France, Jul. 2021. [Online]. Available: https://www.oiv.int/en/oiv-life/table-and-dried-grapes-world-data-available
[6] Z. Sohrabi. (Dec. 2018). Grape Production in Iran's Jowzan Valley Declared Globally Important Agricultural Heritage. Financial Tribune, Iran. Accessed: Aug. 5, 2021. [Online]. Available: https://financialtribune.com/articles/travel/95386/grape-production-in-irans-jowzan-valley-declared-globally-important
[7] D. E. Miliordos, L. Galetto, E. Ferrari, M. Pegoraro, C. Marzachì, and D. Bosco, "Acibenzolar-S-methyl may prevent vector-mediated flavescence dorée phytoplasma transmission, but is ineffective in inducing recovery of infected grapevines," *Pest Manage. Sci.*, vol. 73, no. 3, pp. 534–540, Mar. 2017.
[8] J. Luck, S. K. Pitla, S. A. Shearer, T. G. Mueller, C. R. Dillon, J. P. Fulton, and S. F. Higgins, "Potential for pesticide and nutrient savings via map-based automatic boom section control of spray nozzles," *Comput. Electron. Agricult.*, vol. 70, no. 1, pp. 19–26, Jan. 2010.
[9] S. Pyo, "Actual state of pesticide management and rate of complaints of prevalency subjective symptom in some farmer," M.S. dissertation, Occupational Health Graduate School Public Health, Yonsei Univ., Seoul, South Korea, 2006.
[10] A. S. Paymode and V. B. Malode, "Transfer learning for multi-crop leaf disease image classification using convolutional neural network VGG," *Artif. Intell. Agricul.*, vol. 6, pp. 23–33, Jan. 2022, doi: 10.1016/j.aiia.2021.12.002.
[11] M. A. Islam, M. S. Islam, M. S. Hossen, M. U. Emon, M. S. Keya, and A. Habib, "Machine learning based image classification of papaya disease recognition," in *Proc. 4th Int. Conf. Electron., Commun. Aerosp. Technol. (ICECA)*, Nov. 2020, pp. 1353–1360.
[12] S. Nesteruk, D. Shadrin, M. Pukalchik, A. Somov, C. Zeidler, P. Zabel, and D. Schubert, "Image compression and plants classification using machine learning in controlled-environment agriculture: Antarctic station use case," *IEEE Sensors J.*, vol. 21, no. 16, pp. 17564–17572, Aug. 2021.
[13] F. C. H. Al-Saddik, J. C. Simon, O. Brousse, and F. Cointault, "DAMAV: Un projet interregional de detection de foyers infectieux de flavescence doree par imagerie de drone," *Journée Technique Vitinnov*, pp. 32–35, Feb. 2016.

[14] N. R. Kolhalkar and V. L. Krishnan, "Mechatronics system for diagnosis and treatment of major diseases in grape vineyards based on image processing," *Mater. Today, Proc.*, vol. 23, pp. 549–556, Mar. 2020, doi: 10.1016/j.matpr.2019.05.407.

[15] L. Hashemi-Beni and A. Gebrehiwot, "Deep learning for remote sensing image classification for agriculture applications," *Int. Arch. Photogramm., Remote Sens. Spatial Inf. Sci.*, vols. XLIV-M–2-2020, pp. 51–54, Nov. 2020.

[16] D. Herrera, S. Tosetti, and R. Carelli, "Dynamic modeling and identification of an agriculture autonomous vehicle," *IEEE Latin Amer. Trans.*, vol. 14, no. 6, pp. 2631–2637, Jun. 2016.

[17] (2021). *Dino*. Naio-Technologies, France. Accessed: Jun. 14, 2022. [Online]. Available: https://www.naio-technologies.com,

[18] H. L. Kushwaha, "Robotic and mechatronic application in agriculture," *RASSA. J. Sci. Soc.*, vol. 1, no. 3, pp. 89–97, 2019.

[19] (2022). *Ecorobotix*. Switzerland. Accessed: Jun. 15, 2022. [Online]. Available: https://www.ecorobotix.com/en/autonomous-robot-weeder/

[20] M. Hakim, H. Pratiwi, A. Nugraha, S. Yatmono, A. Wardhana, E. Damarwan, T. Agustianto, and S. Noperi, "Development of unmanned aerial vehicle (UAV) fixed-wing for monitoring, mapping and dropping applications on agricultural land," *J. Phys., Conf.*, vol. 2111, no. 1, Nov. 2021, Art. no. 012051.

[21] K. K. Dhiman, M. Kothari, and Abhishek, "Autonomous control and transportation of underslung load with single and dual lift helicopter systems," *J. Dyn. Syst., Meas., Control*, vol. 144, no. 4, Apr. 2022, Art. no. 041001.

[22] N. Xuan-Mung, S. K. Hong, N. P. Nguyen, L. N. N. T. Ha, and T.-L. Le, "Autonomous quadcopter precision landing onto a heaving platform: New method and experiment," *IEEE Access*, vol. 8, pp. 167192–167202, 2020.

[23] Y.-T. Wu, Z. Qin, A. Eizad, and S.-K. Lyu, "Numerical investigation of the mechanical component design of a hexacopter drone for real-time fine dust monitoring," *J. Mech. Sci. Technol.*, vol. 35, no. 7, pp. 3101–3111, Jul. 2021.

[24] B. Zhang, S. Tsuchiya, and H. Lim, "Development of a lightweight octocopter drone for monitoring complex indoor environment," in *Proc. 6th Asia–Pacific Conf. Intell. Robot Syst. (ACIRS)*, Tokyo, Japan, Jul. 2021, pp. 1–5.

[25] M. Y. Chen, C. S. Gillum, G. C. Lewin, M. S. Sherriff, G. T. Garner, D. H. Edwards, E. L. Boehmer, N. M. Eller, J. T. Slack, C. R. Speck, S. M. Brown, H. G. Williams, and S. H. Wilson, "Designing a spatially aware and autonomous quadcopter," in *Proc. IEEE Syst. Inf. Eng. Design Symp.*, Apr. 2013, pp. 213–218.

[26] K. LaFleur, K. Cassady, A. Doud, K. Shades, E. Rogin, and B. He, "Quadcopter control in three-dimensional space using a noninvasive motor imagery-based brain–computer interface," *J. Neural Eng.*, vol. 10, no. 4, Aug. 2013, Art. no. 046003, doi: 10.1088/1741-2560/10/4/046003.

[27] L. M. Argentim, W. C. Rezende, P. E. Santos, and R. A. Aguiar, "PID, LQR and LQR-PID on a quadcopter platform," in *Proc. Int. Conf. Informat., Electron. Vis. (ICIEV)*, Dhaka, Bangladesh, May 2013, pp. 1–6.

[28] O. O. Patrick, E. O. Nnadi, and H. J. Ajaelu, "Effective use of quadcopter drones for safety and security monitoring in a building construction sites: Case study Enugu Metropolis Nigeria," *J. Eng. Technol. Res.*, vol. 12, no. 1, pp. 37–46, 2020. [Online]. Available: https://academicjournals.org/journal/JETR/article-full-text/84C7C5A65235

[29] R. J. Bunker, J. P. Sullivan, and D. A. Kuhn, "Use of weaponized consumer drones in Mexican crime war," Small Wars J., Counter-IED Rep., 2021, pp. 69–77.

[30] G. Ononiwu, A. Okoye, J. Onojo, and N. Onuekwusi, "Design and implementation of a real time wireless quadcopter for rescue operations," *Amer. J. Eng. Res.*, vol. 5, no. 9, pp. 130–138, 2016.

[31] Y. Gupta, P. Mudgil, V. Sharma, and Z. Hussain. (2022). *DRONES: The Smart Technology in Modern Agriculture*. [Online]. Available: http://dx.doi.org/10.2139/ssrn.4031732

[32] S. Selvaganapathy and A. Ilangumaran, "Design of quadcopter for aerial view and organ transportation using drone technology," *Asian. J. Appl. Sci. Technol. (AJAST)*, vol. 1, no. 3, pp. 311–315, 2017.

[33] A. Merwaday and I. Guvenc, "UAV assisted heterogeneous networks for public safety communications," in *Proc. IEEE Wireless Commun. Netw. Conf. Workshops (WCNCW)*, New Orleans, LA, USA, Mar. 2015, pp. 329–334.

[34] M. I. Varentsov, A. Y. Artamonov, A. D. Pashkin, and I. A. Repina, "Experience in the quadcopter-based meteorological observations in the atmospheric boundary layer," *IOP Conf. Earth Environ. Sci.*, vol. 231, pp. 16–18, May 2019.

[35] S. Alabachi, "Guided autonomy for quadcopter photography," Ph.D. dissertation, Dept. Elect. Comput. Eng., Univ. Central Florida, Gainesville, FL, USA, 2019.

[36] X. Hu, J. Cheng, and H. Luo, "Task assignment for multi-UAV under severe uncertainty by using stochastic multicriteria acceptability analysis," *Math. Problems Eng.*, vol. 2015, pp. 1–10, 2015, doi: 10.1155/2015/249825.

[37] A.-K. Mahlein, "Plant disease detection by imaging sensors–parallels and specific demands for precision agriculture and plant phenotyping," *Plant Disease*, vol. 100, no. 2, pp. 241–251, Feb. 2016, doi: 10.1094/PDIS-03-15-0340-FE.

[38] S. F. Di Gennaro, E. Battiston, S. Di Marco, O. Facini, A. Matese, M. Nocentini, A. Palliotti, and L. Mugnai, "Unmanned aerial vehicle (UAV)-based remote sensing to monitor grapevine leaf stripe disease within a vineyard affected by esca complex," *Phytopathol. Mediterranea*, vol. 55, no. 2, pp. 262–275, Aug. 2016, doi: 10.14601/Phytopathol_Mediterr-18312.

[39] H. S. Abdullahi and R. E. Sheriff, "Introduction to deep learning in precision agriculture: Farm image feature detection using unmanned aerial vehicles through classification and optimization process of machine learning with convolution neural network," in *Deep Learning for Sustainable Agriculture*. Cambridge, MA, USA: Academic Press, 2022, pp. 81–107.

[40] M. M. Petrou and C. Petrou, *Image Processing: The Fundamentals*. Hoboken, NJ, USA: Wiley, 2010.

[41] A. G. T. Schut, P. C. S. Traore, X. Blaes, and R. A. de By, "Assessing yield and fertilizer response in heterogeneous smallholder fields with UAVs and satellites," *Field Crops Res.*, vol. 221, pp. 98–107, May 2018, doi: 10.1016/j.fcr.2018.02.018.

[42] M. Karpina, M. Jarząbek-Rychard, P. Tymków, and A. Borkowski, "UAV-based automatic tree growth measurement for biomass estimation," *Int. Arch. Photogramm., Remote Sens. Spatial Inf. Sci.*, vols. XLI–B8, pp. 685–688, Jun. 2016, doi: 10.5194/isprs-archives-XLI-B8-685-2016.

[43] M. D. Bah, A. Hafiane, and R. Canals, "Weeds detection in UAV imagery using SLIC and the Hough transform," in *Proc. 7th Int. Conf. Image Process. Theory, Tools Appl. (IPTA)*, Montreal, QC, Canada, Nov. 2017, pp. 1–6.

[44] I. Ibrahim and A. Abdulazeez, "The role of machine learning algorithms for diagnosing diseases," *J. Appl. Sci. Technol. Trends*, vol. 2, no. 1, pp. 10–19, Mar. 2021, doi: 10.38094/jastt20179.

[45] S. Meivel, R. Maguteeswaran, N. Gandhiraj, and G. Srinivasan, "Quadcopter UAV based fertilizer and pesticide spraying system," *J. Eng. Sci.*, vol. 1, no. 1, pp. 8–12, 2016.

[46] M. Kerkech, A. Hafiane, and R. Canals, "Deep leaning approach with colorimetric spaces and vegetation indices for vine diseases detection in UAV images," *Comput. Electron. Agricult.*, vol. 155, pp. 237–243, Dec. 2018, doi: 10.1016/j.compag.2018.10.006.

[47] V. Artale, C. L. R. Milazzo, and A. Ricciardello, "Mathematical modeling of hexacopter," *Appl. Math. Sci.*, vol. 7, no. 97, pp. 4805–4811, 2013, doi: 10.12988/ams.2013.37385.

[48] E. Apriaskar, Y. P. Nugraha, and B. R. Trilaksono, "Simulation of simultaneous localization and mapping using hexacopter and RGBD camera," in *Proc. 2nd Int. Conf. Autom., Cognit. Sci., Opt., Micro Electro-Mech. Syst., Inf. Technol. (ICACOMIT)*, Jakarta, Indonesia, Oct. 2017, pp. 48–53.

[49] U. M. Arief, S. Subiyanto, T. Andrasto, S. Sukamta, V. N. Sulistyawan, E. Sarwono, A. A. Alfian, P. Wicaksono, P. N. Amelia, and A. D. H. Putra, "Design of hexacopter UAV system for disinfectant spraying," *IOP Conf. Earth Environ. Sci.*, vol. 700, no. 1, 2021, Art. no. 012023.

[50] A. H. Zakaria, Y. M. Mustafah, M. M. M. Hatta, and M. N. N. Azlan, "Development of load carrying and releasing system of hexacopter," in *Proc. 10th Asian Control Conf. (ASCC)*, Kota Kinabalu, Malaysia, May 2015, pp. 1–6.

[51] S. S. Sannakki, V. S. Rajpurohit, V. B. Nargund, and P. Kulkarni, "Diagnosis and classification of grape leaf diseases using neural networks," in *Proc. 4th Int. Conf. Comput. Ciommun. Netw. Technol. (ICCCNT)*, Tiruchengode, India, Jul. 2013, pp. 1–5.

[52] R. Kaur and S. S. Kang, "An enhancement in classifier support vector machine to improve plant disease detection," in *Proc. IEEE 3rd Int. Conf. MOOCs, Innov. Technol. Educ. (MITE)*, Amritsar, India, Oct. 2015, pp. 135–140.

[53] J. Zhu, A. Wu, X. Wang, and H. Zhang, "Identification of grape diseases using image analysis and BP neural networks," *Multimedia Tools Appl.*, vol. 79, nos. 21–22, pp. 14539–14551, Jun. 2020, doi: 10.1007/s11042-018-7092-0.

[54] A. D. Andrushia and A. T. Patricia, "Artificial bee colony optimization (ABC) for grape leaves disease detection," *Evolving Syst.*, vol. 11, no. 1, pp. 105–117, 2020, doi: 10.1007/S12530-019-09289-2.
[55] Z. Gao, L. R. Khot, R. A. Naidu, and Q. Zhang, "Early detection of grapevine leafroll disease in a red-berried wine grape cultivar using hyperspectral imaging," *Comput. Electron. Agricult.*, vol. 179, Dec. 2020, Art. no. 105807, doi: 10.1016/j.compag.2020.105807.
[56] A. Adeel, M. A. Khan, M. Sharif, F. Azam, J. H. Shah, T. Umer, and S. Wan, "Diagnosis and recognition of grape leaf diseases: An automated system based on a novel saliency approach and canonical correlation analysis based multiple features fusion," *Sustain. Computing: Informat. Syst.*, vol. 24, Dec. 2019, Art. no. 100349, doi: 10.1016/J.SUSCOM.2019.08.002.
[57] A. A. Ahmed and G. H. Reddy, "A mobile-based system for detecting plant leaf diseases using deep learning," *AgriEngineering*, vol. 3, no. 3, pp. 478–493, 2021, doi: 10.3390/agriengineering3030032.
[58] S. Ahmed, M. B. Hasan, T. Ahmed, M. R. K. Sony, and M. H. Kabir, "Less is more: Lighter and faster deep neural architecture for tomato leaf disease classification," *IEEE Access*, vol. 10, pp. 68868–68884, 2022.
[59] Y. Wu, X. Feng, and G. Chen, "Plant leaf diseases fine-grained categorization using convolutional neural networks," *IEEE Access*, vol. 10, pp. 41087–41096, 2022, doi: 10.1109/ACCESS.2022.3167513.
[60] H. Amin, A. Darwish, A. E. Hassanien, and M. Soliman, "End-to-end deep learning model for corn leaf disease classification," *IEEE Access*, vol. 10, pp. 31103–31115, 2022, doi: 10.1109/ACCESS.2022.3159678.
[61] E. Elfatimi, R. Eryigit, and L. Elfatimi, "Beans leaf diseases classification using MobileNet models," *IEEE Access*, vol. 10, pp. 9471–9482, 2022, doi: 10.1109/ACCESS.2022.3142817.
[62] Z. Zinonos, S. Gkelios, A. F. Khalifeh, D. G. Hadjimitsis, Y. S. Boutalis, and S. A. Chatzichristofis, "Grape leaf diseases identification system using convolutional neural networks and Lora technology," *IEEE Access*, vol. 10, pp. 122–133, 2022, doi: 10.1109/ACCESS.2021.3138050.
[63] A. Krizhevsky, I. Sutskever, and G. E. Hinton, "ImageNet classification with deep convolutional neural networks," in *Proc. Adv. Neural Inf. Process. Syst. (NIPS)*, vol. 25, Dec. 2012, pp. 1097–1105, doi: 10.1145/3065386.
[64] C. Szegedy, W. Liu, Y. Jia, P. Sermanet, S. Reed, D. Anguelov, D. Erhan, V. Vanhoucke, and A. Rabinovich, "Going deeper with convolutions," in *Proc. IEEE Conf. Comput. Vis. Pattern Recognit.*, Boston, MA, USA, Jun. 2015, pp. 1–9.
[65] S. Tammina, "Transfer learning using VGG-16 with deep convolutional neural network for classifying images," *Int. J. Sci. Res. Publ. (IJSRP)*, vol. 9, no. 10, pp. 143–150, 2019, doi: 10.29322/IJSRP.9.10.2019.p9420.
[66] K. He, X. Zhang, S. Ren, and J. Sun, "Deep residual learning for image recognition," in *Proc. IEEE Conf. Comput. Vis. Pattern Recognit. (CVPR)*, Jun. 2016, pp. 770–778.
[67] *Downy Mildew*. Amgrow, Australia. Accessed: Jul. 20, 2021. [Online]. Available: https://www.amgrow.com.au/problem/downy-mildew-2
[68] (2017). *Anthracnose of Grapes*. Missouri Botanical Garden, America. Accessed: Sep. 20, 2021. [Online]. Available: https://b2n.ir/t71999
[69] *Powdery Mildew*. Amgrow, Australia. Accessed: Jul. 21, 2021. [Online]. Available: https://www.amgrow.com.au/problem/powdery-mildew
[70] S. Mousavi and G. Farahani, "Introducing a new method of automatic cleaning of the PV array surface using a suction robot," *Mechatronics*, vol. 85, Aug. 2022, Art. no. 102845.
[71] (2020). *Differential GPS*. DYNO Noble, Americas. Accessed: Oct. 1, 2021. [Online]. Available: https://www.dynonobel.com/practical-innovations/recent-innovation/differential-gps
[72] G. Lin, Y. Tang, X. Zou, J. Xiong, and Y. Fang, "Color-, depth-, and shape-based 3D fruit detection," *Precis. Agricult.*, vol. 21, no. 1, pp. 1–17, Feb. 2020.
[73] G. Farahani, "Dynamic and robust method for detection and locating vehicles in the video images sequences with use of image processing algorithm," *EURASIP J. Image Video Process.*, vol. 2017, no. 1, pp. 1–22, Dec. 2017.
[74] Y. Tian, G. Yang, Z. Wang, H. Wang, E. Li, and Z. Liang, "Apple detection during different growth stages in orchards using the improved YOLO-V3 model," *Comput. Electron. Agricult.*, vol. 157, pp. 417–426, Feb. 2019, doi: 10.1016/j.compag.2019.01.012.
[75] Y. Wang, Q. Chen, and B. Zhang, "Image enhancement based on equal area dualistic sub-image histogram equalization method," *IEEE Trans. Consum. Electron.*, vol. 45, no. 1, pp. 68–75, Feb. 1999, doi: 10.1109/30.754419.
[76] H. Jiang and E. Learned-Miller, "Face detection with the faster R-CNN," in *Proc. 12th IEEE Int. Conf. Autom. Face Gesture Recognit. (FG)*, Washington, DC, USA, May 2017, pp. 650–657.
[77] S. Ren, K. He, R. Girshick, and J. Sun, "Faster R-CNN: Towards real-time object detection with region proposal networks," *IEEE Trans. Pattern Anal. Mach. Intell.*, vol. 39, no. 6, pp. 1137–1149, Jun. 2017, doi: 10.1109/TPAMI.2016.2577031.
[78] A. Abdalla, H. Cen, L. Wan, R. Rashid, H. Weng, W. Zhou, and Y. He, "Fine-tuning convolutional neural network with transfer learning for semantic segmentation of ground-level oilseed rape images in a field with high weed pressure," *Comput. Electron. Agricult.*, vol. 167, Dec. 2019, Art. no. 105091.
[79] Z. Zhang, A. K. Pothula, and R. Lu, "A review of bin filling technologies for apple harvest and postharvest handling," *Appl. Eng. Agricult.*, vol. 34, no. 4, pp. 687–703, 2018, doi: 10.13031/aea.12827.
[80] M. Lin, Q. Chen, and S. Yan, "Network in network," 2013, *arXiv:1312.4400*.
[81] S. Ioffe and C. Szegedy, "Batch normalization: Accelerating deep network training by reducing internal covariate shift," in *Proc. 32nd Int. Conf. Mach. Learn.*, Lille, France, 2015, pp. 448–456.
[82] B. Kohlhepp, "Deep learning for computer vision with Python," *Comput. Rev.*, vol. 61, no. 1, pp. 9–10, 2020.
[83] P. F. Felzenszwalb, R. B. Girshick, D. McAllester, and D. Ramanan, "Object detection with discriminatively trained part-based models," *IEEE Trans. Pattern Anal. Mach. Intell.*, vol. 32, no. 9, pp. 1627–1645, Sep. 2010, doi: 10.1109/TPAMI.2009.167.

SEYEDAMIRHOSSEIN MOUSAVI was born in June 1995. He received the bachelor's degree in electronics engineering and the master's degree in mechatronics engineering. He has cooperated in several research projects with the Iranian Research Organization for Science and Technology (IROST). His research interests include mechatronics, robotics, smart and soft actuators, quadcopters, and image processing.

GHOLAMREZA FARAHANI received the B.Sc. degree in electrical engineering from the Sharif University of Technology, Tehran, Iran, in 1998, and the M.Sc. and Ph.D. degrees in electrical engineering from the Amirkabir University of Technology (Polytechnic), Tehran, in 2000 and 2006, respectively. He is currently an Associate Professor with the Electrical Engineering and Information Technology Department, Iranian Research Organization for Science and Technology (IROST), Iran. His research interests include signal processing, especially image processing.